Genetic deletion of p66^{Shc} adaptor protein prevents hyperglycemia-induced endothelial dysfunction and oxidative stress

Giovanni G. Camici*, Marzia Schiavoni*, Pietro Francia†, Markus Bachschmid‡, Ines Martin-Padura§, Martin Hersberger¶, Felix C. Tanner*, PierGiuseppe Pelicci§, Massimo Volpe†‖, Piero Anversa**, Thomas F. Lüscher*, and Francesco Cosentino*†,††

*Cardiology and Cardiovascular Research, University Hospital, Zürich, Institute of Physiology, University of Zürich, CH-8057 Zürich, Switzerland; †Division of Cardiology, Second Faculty of Medicine, University La Sapienza, 00189 Rome, Italy; ‡Department of Biology, University of Konstanz, D-78457 Konstanz, Germany; §Department of Experimental Oncology, European Institute of Oncology, 20141 Milan, Italy; ¶Institute of Clinical Chemistry, University Hospital, CH-8057 Zürich, Switzerland; **New York Medical College, Cardiovascular Research Institute, Valhalla, NY 10595; and ‖IRCCS Neuromed, 86077 Pozzilli, Italy

Edited by Louis J. Ignarro, University of California School of Medicine, Los Angeles, CA, and approved February 5, 2007 (received for review October 31, 2006)

Increased production of reactive oxygen species (ROS) and loss of endothelial NO bioavailability are key features of vascular disease in diabetes mellitus. The p66^{Shc} adaptor protein controls cellular responses to oxidative stress. Mice lacking p66^{Shc} (p66$^{Shc-/-}$) have increased resistance to ROS and prolonged life span. The present work was designed to investigate hyperglycemia-associated changes in endothelial function in a model of insulin-dependent diabetes mellitus p66$^{Shc-/-}$ mouse. p66$^{Shc-/-}$ and wild-type (WT) mice were injected with citrate buffer (control) or made diabetic by an i.p. injection of 200 mg of streptozotocin per kg of body weight. Streptozotocin-treated p66$^{Shc-/-}$ and WT mice showed a similar increase in blood glucose. However, significant differences arose with respect to endothelial dysfunction and oxidative stress. WT diabetic mice displayed marked impairment of endothelium-dependent relaxations, increased peroxynitrite (ONOO$^-$) generation, nitrotyrosine expression, and lipid peroxidation as measured in the aortic tissue. In contrast, p66$^{Shc-/-}$ diabetic mice did not develop these high-glucose-mediated abnormalities. Furthermore, protein expression of the antioxidant enzyme heme oxygenase 1 and endothelial NO synthase were up-regulated in p66$^{Shc-/-}$ but not in WT mice. We report that p66$^{Shc-/-}$ mice are resistant to hyperglycemia-induced, ROS-dependent endothelial dysfunction. These data suggest that p66^{Shc} adaptor protein is part of a signal transduction pathway relevant to hyperglycemia vascular damage and, hence, may represent a novel therapeutic target against diabetic vascular complications.

Endothelial dysfunction is an early feature of diabetic vascular disease, characterized by a decrease in nitric oxide (NO) bioavailability and a concomitant increase in vascular superoxide (O_2^-) formation (1). Loss of NO bioavailability precedes the development of overt atherosclerosis and is an independent predictor of adverse cardiovascular events (2, 3). The reaction of O_2^- with NO leads to production of peroxynitrite (ONOO$^-$). ONOO$^-$ easily penetrates across the phospholipid membrane and produces substrate nitration, thereby inactivating regulatory receptors and enzymes such as free-radical scavengers (4, 5). Indeed, enhanced production of reactive oxygen species (ROS) has been recognized as a major determinant of hyperglycemia-induced endothelial dysfunction (6, 7). The mammalian adaptor protein ShcA has three isoforms with relative molecular masses of 46, 52, and 66 kDa. The three isoforms share an Src-homology 2 domain, a collagen-homology region, and a phosphotyrosine-binding domain. Recent studies have suggested distinct physiological roles for the three Shc isoforms. Both p46^{Shc} and p52^{Shc} promote cell proliferation and differentiation through RAS and the MAP kinases (8), whereas p66^{Shc}, by virtue of its unique NH_2-terminal collagen homology 2 (CH_2) region, controls oxidative stress responses and life span. In fact, embryo fibroblasts from mice carrying a targeted mutation of p66^{Shc} (p66$^{Shc-/-}$) were found to be protected from loss of cell viability induced by oxidative stress (9). Furthermore, p66$^{Shc-/-}$ mice have an ≈30% increase in life span and exhibit less atherosclerosis during a high-fat diet, suggesting that p66^{Shc} is involved in aging and aging-associated disease (9, 10). Accordingly, we demonstrated that old p66$^{Shc-/-}$ mice maintain acetylcholine-induced relaxations compared with age-matched wild-type (WT) littermates (11). In addition, p66$^{Shc-/-}$ cells exhibit reduced levels of intracellular ROS as well as decreased mitochondrial DNA alterations, indicating that p66^{Shc} is a critical component of the intracellular redox state (12).

Although the exact biochemical role of p66^{Shc} remains to be determined, p66^{Shc} was shown to act as a downstream target of the tumor suppressor protein p53 and is indispensable for its ability to induce elevations of intracellular oxidants and apoptosis (13). Recently, p66^{Shc} was shown to participate in mitochondrial ROS production by serving as a redox-sensitive enzyme that oxidizes cytochrome *c*, thus generating proapoptotic ROS in response to specific stress signals (12–15). These data support the concept that p66^{Shc} plays a pivotal role in controlling oxidative stress and participates in the pathogenesis of vascular disease. Mitochondrial O_2^- production has also been recognized as an important mediator of hyperglycemic vascular damage (16). In this regard, p66^{Shc} gene expression is increased significantly in peripheral blood monocytes obtained from patients with diabetes mellitus and is correlated with plasma isoprostanes, an *in vivo* marker of oxidative stress (17). Furthermore, diabetic glomerulopathy is less pronounced in p66$^{Shc-/-}$ mice (18). These findings prompted us to investigate whether p66$^{Shc-/-}$ mice are protected against hyperglycemia-induced, ROS-mediated endothelial dysfunction.

Results

Induction of Diabetes with Streptozotocin (STZ). Baseline fasting glucose levels, total cholesterol, triglycerides, and glycated hemo-

Author contributions: G.G.C. and M.S. contributed equally to this work. G.G.C., M.S., T.F.L., and F.C. designed research; G.G.C., M.S., M.B., and M.H. performed research; I.M.-P., M.H., F.C.T., P.P., M.V., and P.A. contributed new reagents/analytic tools; G.G.C., M.S., P.F., M.B., I.M.-P., M.H., F.C.T., P.P., M.V., P.A., and F.C. analyzed data; and G.G.C., P.F., P.P., P.A., T.F.L., and F.C. wrote the paper.

The authors declare no conflict of interest.

This article is a PNAS direct submission.

Abbreviations: Cu/ZnSOD, copper/zinc superoxide dismutase; eNOS, endothelial nitric oxide synthase; HbA1c, glycated hemoglobin; HO, heme oxygenase; HO-1, heme oxygenase 1; L-NAME, l-N^G-nitro-L-arginine methyl ester; MnSOD, manganese superoxide dismutase; ONOO$^-$, peroxynitrite; ROS, reactive oxygen species; STZ, streptozotocin; TBARS, thiobarbituric acid-reactive substances.

††To whom correspondence should be addressed at: Cardiology and Cardiovascular Research, University of Zürich-Irchel, Winterthurerstrasse, 190, CH-8057 Zürich, Switzerland. E-mail: f_cosentino@hotmail.com.

Table 1. Biochemical data from p66$^{Shc-/-}$ and WT littermates, 4 weeks after induction of diabetes using STZ (diabetic) or after buffer injection (control)

	WT		p66$^{Shc-/-}$	
	Control	Diabetic	Control	Diabetic
Glucose, mmol/liter	5.3 ± 0.2	25.6 ± 1.87*	5.6 ± 0.08	27.3 ± 2.03*
HbA1c, %	1.2 ± 0.7	3 ± 0.4*	1.0 ± 0.1	3.0 ± 0.7*
Total cholesterol, mmol/liter	3.9 ± 0.2	5.5 ± 1*	3.8 ± 0.4	6.7 ± 0.2*
Triglycerides, mmol/liter	1.5 ± 0.3	2.4 ± 1.5	1.3 ± 0.3	3.4 ± 0.5

Values are mean ± SEM. $n = 6–9$ in each group. *, $P < 0.05$ vs. control WT and p66$^{Shc-/-}$ mice.

globin (HbA1c) were comparable in p66$^{Shc-/-}$ and WT mice. In preliminary experiments, a single i.p. injection of STZ (200 mg/kg) resulted in sustained blood glucose concentrations of >20 mmol/liter in >80% of mice without differences between WT and p66$^{Shc-/-}$ mice. STZ treatment significantly increased glucose, HbA1c, and cholesterol levels in WT and p66$^{Shc-/-}$ mice compared with citrate buffer controls (Table 1).

Effect of STZ-Induced Diabetes on p66^{Shc} Expression. To elucidate the effects of high glucose on p66^{Shc} protein, we investigated its expression pattern in lysed aortas from control and diabetic WT mice. p66^{Shc} protein was significantly up-regulated in WT mice after induction of diabetes by STZ compared with controls (Fig. 1). Both control and diabetic p66$^{Shc-/-}$ mice did not display any expression of p66^{Shc} protein (Fig. 1).

Endothelial Function in Diabetic Aortas. Isometric tension studies demonstrated no difference in vascular contractions to norepinephrine between aortas obtained from diabetic and nondiabetic WT or p66$^{Shc-/-}$ mice (Table 2). However, endothelium-dependent relaxations to acetylcholine were significantly impaired in diabetic WT mice compared with controls (Table 2 and Fig. 2). In contrast, endothelium-dependent relaxations remained normal in diabetic p66$^{Shc-/-}$ mice, suggesting a preserved NO bioavailability (Fig. 2). Indeed, inhibition of NO synthase with L-N^G-nitroarginine methyl ester (L-NAME) abolished the relaxations to acetylcholine in diabetic p66$^{Shc-/-}$ mice (Table 2). Endothelium-independent relaxations to the NO donor sodium nitroprusside were identical in all groups, denoting no differences in vascular smooth muscle responses to NO (Table 2).

STZ-Induced Diabetes and Oxidative Stress. To determine hyperglycemia-induced vascular oxidative stress, we measured $ONOO^-$ generation by chemiluminescence as well as 3-nitrotyrosine residues by immunohistochemistry in aortic tissue from all groups. $ONOO^-$ levels in control p66$^{Shc-/-}$ were lower than in WT mice (Fig. 3). Further, and in agreement with preserved NO bioavailability, the hyperglycemia-induced generation of $ONOO^-$ observed in WT did not occur in p66$^{Shc-/-}$ mice (Fig. 3). Because $ONOO^-$ leads to increased protein 3-nitrotyrosine content, we analyzed 3-nitrotyrosine levels in lysed aortas by immunostaining. Diabetic p66$^{Shc-/-}$ mice exhibited a markedly reduced immunoreactivity both in the endothelium and in the media compared with diabetic WT (Fig. 3). This favorable redox profile was confirmed by aortic thiobarbituric acid-reactive substances (TBARS) levels assessment, showing that p66$^{Shc-/-}$ mice had lower lipid peroxidation both in basal conditions and in the high-glucose setting compared with WT mice (Fig. 4).

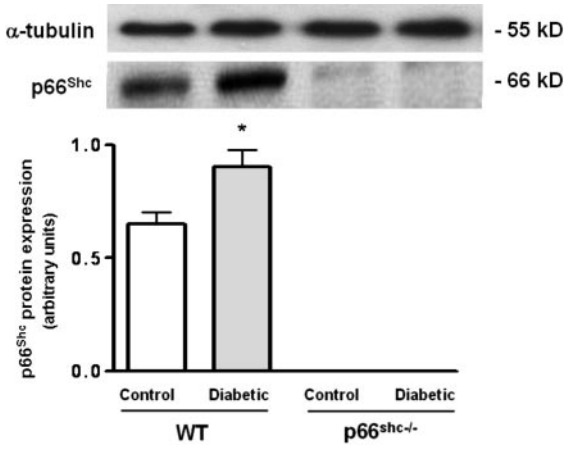

Fig. 1. p66^{Shc} protein expression in aortic lysates from WT control and diabetic mice. Bar graphs show densitometric analysis of Western blot of p66^{Shc} protein in control and diabetic WT and p66$^{Shc-/-}$ mice. α-Tubulin was used as a reference protein. Data are presented as mean ± SEM; $n = 3$ in each group. *, $P < 0.05$ vs. control WT mice.

Free-Radical Scavengers. Protein expression of three pivotal free-radical scavengers was assessed to determine whether an up-regulation of antioxidant defense mechanisms might contribute to explain the preserved NO bioavailability in p66$^{Shc-/-}$ diabetic mice. Although manganese superoxide dismutase (MnSOD) and copper/zinc superoxide dismutase (Cu/ZnSOD) were comparable in all of the experimental groups (Fig. 5 *Left* and *Right*, respectively), heme oxygenase 1 (HO-1) was significantly up-regulated in control and diabetic p66$^{Shc-/-}$ mice (Fig. 6 *Left*). Accordingly, a similar pattern was observed for HO activity (Fig. 6 *Right*).

Endothelial Nitric Oxide Synthase (eNOS) Expression and Activity. We assessed the effect of diabetes on eNOS protein expression and activity in p66$^{Shc-/-}$ and WT mice treated with STZ or STZ vehicle buffer (control). The level of protein expressed in control p66$^{Shc-/-}$ mice compared with WT littermates was slightly yet significantly higher. STZ-induced diabetes caused an up-regulation of eNOS in both groups (Fig. 7). However, the relative increase of eNOS protein levels in diabetic p66$^{Shc-/-}$ was 2-fold higher than in diabetic WT mice (Fig. 7). Enzyme activity was not different in the two animal groups under control conditions (Fig. 8). However, in line with the marked protein up-regulation, NOS activity was significantly greater in diabetic p66$^{Shc-/-}$ compared with diabetic WT mice (Fig. 8).

Discussion

This work demonstrates that genetic deletion of p66^{Shc} protein protects diabetic mice from hyperglycemia-induced, ROS-mediated endothelial dysfunction, suggesting that p66^{Shc} is part of a signal transduction pathway relevant to hyperglycemic vascular damage. Several lines of evidence support our conclusion. In WT mice, the expression of p66^{Shc} was up-regulated after induction of diabetes with STZ. Diabetic p66$^{Shc-/-}$ mice did not show any impairment of endothelium-dependent relaxation to acetylcholine compared with WT, and $ONOO^-$ generation was markedly reduced in these animals. Lower $ONOO^-$ levels in diabetic p66$^{Shc-/-}$ mice were associated with a decreased protein nitration and lipid peroxidation. Accordingly, the expression and activity of the antioxidant enzyme HO-1 were increased in p66$^{Shc-/-}$ compared with WT mice. On the other hand, deletion of the p66^{Shc} gene did not

Table 2. Comparison of vasomotor responses in control and diabetic WT and p66$^{Shc-/-}$ mice

	WT		p66$^{Shc-/-}$	
	Control	Diabetic	Control	Diabetic
Maximal contraction to NE (10^{-6} mol/liter), g	1.4 ± 0.04	1.5 ± 0.06	1.5 ± 0.04	1.4 ± 0.02
Maximal relaxations				
Acetylcholine, %	61 ± 3	37 ± 5*	67 ± 6	79 ± 4
Control in the presence of L-NAME (3×10^{-4} mol/liter)	0.9 ± 0.9	−3.4 ± 2.4	2.1 ± 1.3	−2.3 ± 1.3
−Log EC_{50}	7 ± 0.07	6.7 ± 0.02*	7.2 ± 0.02	7.4 ± 0.1
SNP, %	100	100	100	100

NE, norepinephrine; SNP, sodium nitroprusside; +, contraction; −, relaxation. Values are mean ± SEM; $n = 6–9$ in each group. Relaxations are expressed as percent change of contractions to NE (10^{-6} mol/liter). *, $P < 0.05$ vs. control WT and p66$^{Shc-/-}$ mice.

affect either rate of diabetes induction or severity of hyperglycemia after STZ injection. Indeed, blood glucose and HbA1c levels were similar in p66$^{Shc-/-}$ and WT mice. Thus, we could rule out that differences observed among the two groups were caused by different experimental conditions.

Bioavailability of NO is a key marker of vascular health. Endothelial dysfunction, reflected by impaired endothelium-dependent relaxation, occurs in cellular and experimental models of diabetes (6, 19, 20). Similarly, many clinical studies have found that endothelium-dependent vasodilation is abnormal in patients with type 1 or type 2 diabetes (20–22). Hence, decreased levels of NO in diabetes may underlie its atherogenic predisposition. Hyperglycemia induces a series of cellular events that increase the production of ROS and inactivate NO to form $ONOO^-$ (7). Acetylcholine-induced relaxation did not differ in p66$^{Shc-/-}$ and WT mice in control conditions. After induction of diabetes, only WT mice developed marked endothelial dysfunction. These findings are in line with our previous work showing that aged p66$^{Shc-/-}$ mice do not develop endothelial dysfunction compared with WT (11).

Diabetes-induced oxidative stress has been attributed to various biochemical pathways including PKC activation and accelerated electron flow through the mitochondrial respiratory chain (6, 7, 15). p66^{Shc} regulatory protein plays a pivotal role in controlling the intracellular redox state (15). Interestingly, p66^{Shc} gene expression is increased in peripheral blood monocytes obtained from diabetic patients likewise plasma isoprostane levels, an *in vivo* marker of oxidative stress (17). In keeping with these findings, we found that p66^{Shc} adaptor protein is up-regulated in aortas of diabetic mice, suggesting an involvement of the p66^{Shc} pathway in hyperglycemia-induced ROS production. Proapoptotic signals increase cytosolic and mitochondrial p66^{Shc} pools (12, 15). Indeed, these signals release the mitochondrial pool from a high-molecular weight inhibitory complex (13), enabling p66^{Shc} to oxidize cytochrome *c* and, hence, generate ROS (15). Diabetes, through several mechanisms, including hyperglycemia, PKC activation, and oxidative stress, provides these apoptotic signals (23). Recently, gene delivery of Tim44, a component of the high-molecular weight complex that inactivates p66^{Shc} within the mitochondrion, was found to normalize increased ROS generation and enhanced proliferation in smooth muscle cells exposed to high glucose and to improve inflammatory response and neointimal proliferation in the balloon-injured carotid artery of diabetic rats (24). Therefore, p66^{Shc} not only mediates oxidant-induced apoptosis but also regulates intracellular ROS levels. In the diabetic state, the expression and activity of p66^{Shc} could be enhanced by induction of a sustained mitochondrial ROS overproduction or PKC-dependent activation. There is indeed evidence that p66^{Shc} acts as a downstream target after PKC activation by different apoptotic and inflammatory stimuli (M. Giorgio and P.G.P., unpublished observations). Accordingly, the

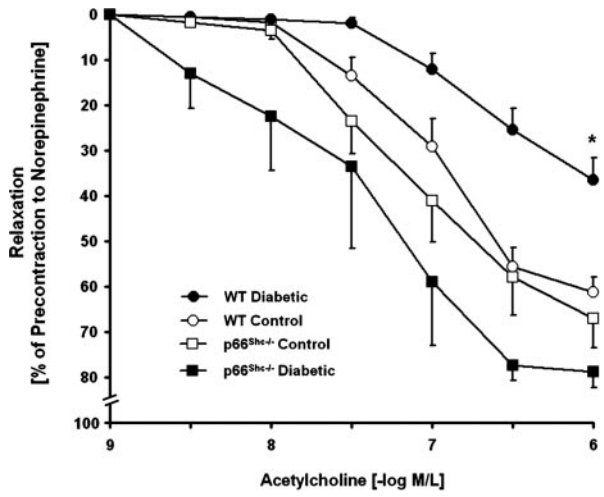

Fig. 2. Isometric tension studies in aortic rings from control and diabetic WT and p66$^{Shc-/-}$ mice. Vessel relaxations to the endothelium-dependent agonist acetylcholine were normal in control WT (open circles) and p66$^{Shc-/-}$ (open squares) mice. Diabetic WT mice (filled circles) exhibited impaired endothelium-dependent relaxations compared with diabetic p66$^{Shc-/-}$ mice (filled squares) and with control WT mice (open circles). There were no differences in endothelium-dependent relaxations between diabetic and control p66$^{Shc-/-}$ mice. Relaxations were obtained during contractions to 10^{-6} mol/liter norepinephrine. Data are presented as mean ± SEM; $n = 6–9$ in each group. *, $P < 0.05$ for diabetic WT mice vs. all other groups.

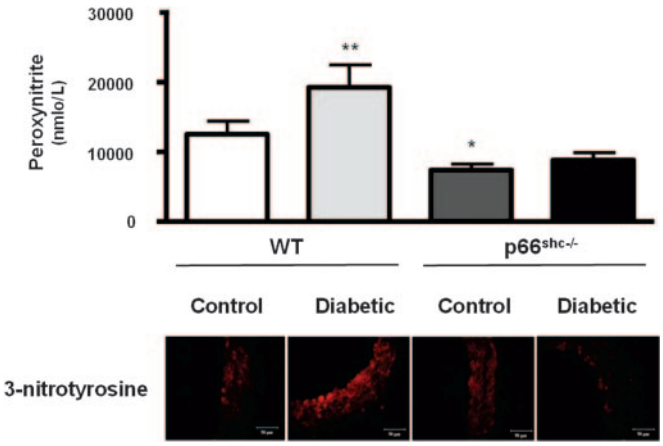

Fig. 3. Bar graphs show $ONOO^-$ levels determined by chemiluminescence. Results are presented as mean ± SEM; $n = 6$ in each group. *, $P < 0.05$ vs. control WT mice; **, $P < 0.05$ vs. control WT mice. Immunostaining of nitrotyrosine residues in aortas from control and diabetic WT and p66$^{Shc-/-}$ mice is shown.

PHYSIOLOGY

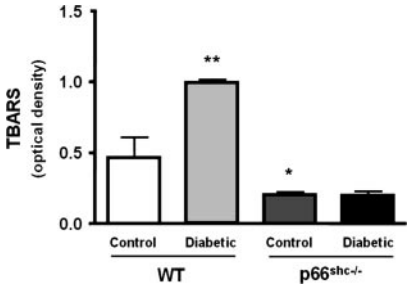

Fig. 4. TBARS levels. Bar graphs show TBARS levels in aortas from control and diabetic WT and $p66^{Shc-/-}$ mice. Results are presented as mean ± SEM; $n = 4$ in each group. *, $P < 0.05$ vs. control WT mice; **, $P < 0.05$ vs. control WT.

prevention of high-glucose-induced ROS generation by inhibitors of PKC, NADPH oxidase, and mitochondrial respiratory chain indicate that both cytosolic and mitochondrial mechanisms contribute to oxidative stress under hyperglycemic conditions. Thus, the fact that in $p66^{Shc-/-}$ diabetic mice we observed lower ROS generation suggests that $p66^{Shc}$ modulates this process at both levels.

Moreover, 3-nitrotyrosine residues, typical end products of the reaction of $ONOO^-$ with biological compounds (1), did not increase in diabetic $p66^{Shc-/-}$ mice. Although nitrotyrosine immunoreactivity was detected in both endothelial and smooth muscle cells of diabetic animals, aortas from diabetic WT mice exhibited markedly enhanced immunostaining compared with $p66^{Shc-/-}$ mice. Because by promoting lipid peroxidation $ONOO^-$ contributes to atherogenesis (25), we also measured TBARS in aortic tissue as a marker of *in vivo* lipid peroxidation (26). $p66^{Shc-/-}$ mice showed lower basal levels of TBARS compared with WT. In contrast to diabetic WT mice, $p66^{Shc-/-}$ mice did not show increased TBARS aortic tissue levels in response to diabetes, thus indicating almost complete protection against lipid peroxidation.

To investigate whether the preserved endothelial function in diabetic $p66^{Shc-/-}$ mice was associated with an up-regulation of antioxidant defense proteins, we also assessed the expression and activity of MnSOD, Cu/ZnSOD, and HO-1. Western blot analysis did not reveal any difference in expression of any SOD isoforms. However, HO-1 protein expression and activity were significantly increased in $p66^{Shc-/-}$ mice compared with WT mice. Previous studies demonstrated that overexpression of the HO-1 gene in human, rabbit, and rat endothelial cells provides protection against oxidative stress (27, 28), underscoring the cytoprotective role of HO-1 (29–31). On the contrary, it was shown that in mice or in humans lacking functional HO-1, the levels of oxidants and oxidative stress-mediated cell injury are increased (32–34). In addition, up-regulation of HO-1 reduces ROS levels by decreasing O_2^- generation itself (27, 35).

In contrast to a previous study from our group investigating the effects of aging in $p66^{Shc-/-}$ mice (11), here we observed that eNOS protein expression was slightly higher in control $p66^{Shc-/-}$ compared with WT mice. The genetic background (129Sv) of WT and $p66^{Shc-/-}$ mice is the same in both studies, and their mean age is comparable. STZ-induced diabetes caused an up-regulation of eNOS in both groups. Importantly, however, the hyperglycemia-induced up-regulation of eNOS expression found in diabetic $p66^{Shc-/-}$ was 2-fold higher than in diabetic WT mice. In line with the marked protein up-regulation, enzyme activity was significantly greater in diabetic $p66^{Shc-/-}$ compared with diabetic WT mice. In contrast, NOS activity was not different in the two animal groups under control conditions, suggesting that the contradictory finding with our previous study might be caused by biological variability of eNOS expression and does not translate into changes of catalytic activity. Such hyperglycemia-induced up-regulation of NO pathway (higher enzyme expression and activity) associated with the inhibitory effect of L-NAME on normal vasorelaxation to acetylcholine clearly indicates a preserved NO bioavailability in diabetic $p66^{Shc-/-}$ mice.

Although we did not investigate how deletion of $p66^{Shc}$ elicits concomitant up-regulation of HO-1 and NO systems, it is conceivable that these events may contribute to protect against glucose-mediated abnormalities in $p66^{Shc-/-}$ mice.

In conclusion, we report that targeted mutation of $p66^{Shc}$ protects against hyperglycemia-induced, ROS-dependent endothelial dysfunction. Thus, it appears that $p66^{Shc}$, by controlling cytosolic and mitochondrial high-glucose-induced changes of the redox state, regulates ROS production and accumulation under this condition. In agreement with previous reports (12, 14, 18, 36), lower levels of intracellular ROS generation were measured in $p66^{Shc-/-}$ mice after induction of diabetes. On the other hand, as observed here in diabetic WT animals, overexpression of $p66^{Shc}$ has been demonstrated in conditions associated with increased levels of oxidative stress as well as ROS-mediated cell death, including experimental dilated cardiomyopathy (37), hindlimb ischemia (36), as well as patients with type 2 diabetes (17). Undoubtedly, the mechanisms of $p66^{Shc}$-dependent signaling require further investigation. However, $p66^{Shc}$ represents a promising therapeutic target to prevent development and progression of diabetic vascular disease.

Materials and Methods

Animals. Forty $p66^{Shc-/-}$ and 40 WT male mice all 129Sv background aged 4–6 months were obtained from the Department of Experimental Oncology of the European Institute of Oncology (Milan, Italy). Mice were housed in temperature-controlled cages (20–22°C), fed ad libitum, and maintained on a 12:12-h light/dark cycle. Study design and experimental protocols were approved by the Institutional Animal Care Committee (Kommission für Tierversuche des Kantons Zürich, Switzerland).

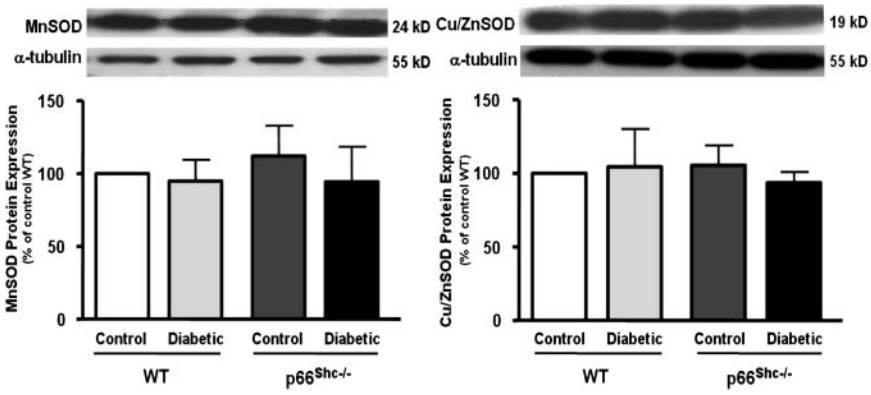

Fig. 5. Protein expression from aortas of control and diabetic WT and $p66^{Shc-/-}$ mice. (*Left*) MnSOD. (*Right*) Cu/ZnSOD. Bar graphs show densitometric analysis of Western blots of MnSOD and Cu/ZnSOD in control and diabetic WT and $p66^{Shc-/-}$ mice, respectively. Results are presented as mean ± SEM; $n = 4–6$ in each group.

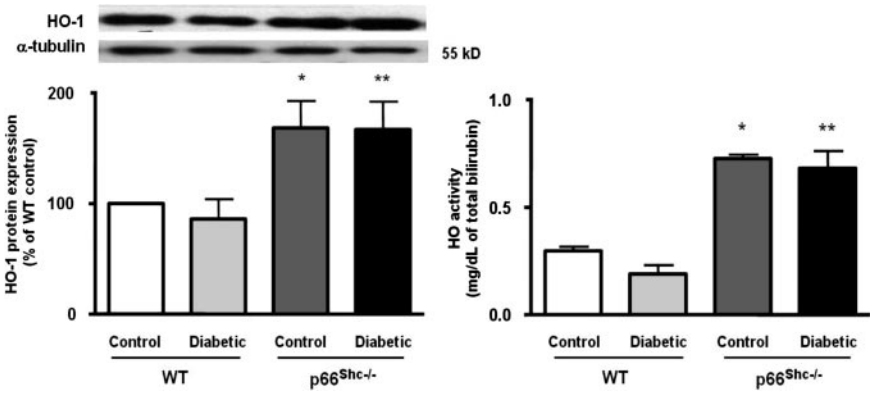

Fig. 6. HO-1 protein expression and total HO activity from aortas of control and diabetic WT and $p66^{Shc-/-}$ mice. (*Left*) HO-1 protein expression from aortas of control and diabetic WT and $p66^{Shc-/-}$ mice. Bar graphs show densitometric analysis of Western blots of HO-1 protein in control and diabetic WT and $p66^{Shc-/-}$ mice. (*Right*) HO activity in control and diabetic WT and $p66^{Shc-/-}$ mice. Results are presented as mean ± SEM; $n = 4$ in each group. *, $P < 0.05$ vs. control WT mice; **, $P < 0.05$ vs. diabetic WT mice.

Induction of Diabetes by STZ Injection. A single high-dose STZ regimen was used to induce pancreatic islet cell destruction and persistent hyperglycemia. STZ (200 mg/kg; Sigma–Aldrich, St. Louis, MO) was freshly dissolved in sterile 0.025 M citrate buffer (pH 4.5) and injected within 10 min. Mice received a single 200 mg/kg i.p. injection of STZ or citrate buffer (control). Blood glucose was monitored weekly by using a sip-in sampling glucose meter (Glucometer Elite XL, Bayer, Laubach, Germany). Hyperglycemia was defined as a random blood glucose level of >200 mg/dl for >3 weeks after STZ injection. Four weeks after treatment, mice were anesthetized by i.p. administration of 50 mg/kg sodium pentobarbital (Butler, Columbus, OH) and then were euthanized. The chest and abdomen were opened with a medial sternotomy. The entire aorta from the heart to the iliac bifurcation was excised and placed in cold Krebs–Ringer bicarbonate solution (pH 7.4 at 37°C, 95% O_2/5% CO_2) of the following composition (mmol/liter): 118.6 NaCl/4.7 KCl/2.5 $CaCl_2$/1.2 KH_2PO_4/1.2 $MgSO_4$/25.1 $NaHCO_3$/11.1 glucose/0.026 calcium EDTA. The aorta was then cleaned of adhering tissue under a dissection microscope, frozen in liquid nitrogen, and stored at −80°C, or used immediately for organ chamber experiments and measurement of ROS production according to the study protocol. Blood samples were collected into chilled EDTA-coated tubes for lipid profile determination and HbA1c dosage. The HbA1c, total cholesterol, and triglyceride contents of blood samples were measured by using commercially available kits (Sigma–Aldrich).

Organ Chamber Experiments. Aortas were cut into rings (2–3 mm long). Each ring was connected to an isometric force transducer (MultiMyograph 610M; Danish Myo Technology, Aarhus, Denmark), suspended in an organ chamber filled with 5 ml of control solution (37°C, pH 7.4), and bubbled with 95% O_2/5% CO_2. Isometric tension was recorded continuously. After a 30-min equilibration period, rings were gradually stretched to the optimal point of their length–tension curve as determined by the contraction in response 60 mM KCl. Concentration-dependent contractions were established by using norepinephrine (10^{-9} to 10^{-5} mol/liter; Sigma–Aldrich). Concentration–response curves were obtained in a cumulative fashion. Several rings cut from the same artery were studied in parallel. Responses to acetylcholine (10^{-9} to 10^{-6} mol/liter; Sigma–Aldrich) in the presence and in the absence of L-NAME (3×10^4 mol/liter; Sigma–Aldrich) were obtained during submaximal contraction to NE. The NO donor sodium nitroprusside (10^{-10} to 10^{-5} mol/liter; Sigma–Aldrich) was added to test endothelium-independent relaxations. Relaxations were expressed as a percentage of the precontracted tension.

Determination of $p66^{Shc}$, eNOS, SOD, and HO-1 by Western Blotting. Aortas were isolated and snap-frozen in liquid nitrogen. Frozen samples were successively pulverized and dissolved in lysis buffer. Equal amounts of proteins (30 μg/lane) were loaded on a separating denaturing SDS/10% polyacrylamide gel and run overnight. Proteins were then transferred onto an activated PVDF membrane (Millipore, Zvg, Switzerland). After blocking for 1 h in 5% milk powder solution, membranes were incubated with the appropriate antibody concentration diluted in 5% milk powder [anti-eNOS rabbit polyclonal antibody mouse monoclonal antibody (1:1,000; Santa Cruz Biotechnology, Santa Cruz, CA), anti-MnSOD rabbit polyclonal antibody (1:2,000; Upstate Biotechnology, Lake Placid, NY), anti-Cu/ZnSOD rabbit polyclonal antibody (1:2,000; Upstate Biotechnology), anti-$p66^{Shc}$ (1:1,000; Upstate Biotechnology), anti-HO-1 rabbit polyclonal antibody (1:2,000; Stressgen Biotechnology, Victoria, Canada)] for 1 h at room temperature. Membranes were then washed and incubated with secondary antibody [horseradish

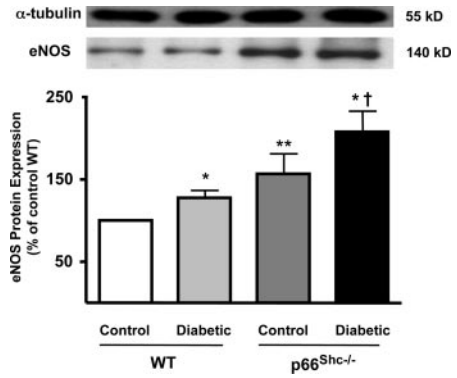

Fig. 7. eNOS protein expression from aortas of control and diabetic WT and $p66^{Shc-/-}$ mice. Bar graphs show densitometric analysis of Western blots of eNOS protein in control and diabetic WT and $p66^{Shc-/-}$ mice. Results are presented as mean ± SEM; $n = 6$–9 in each group. *, $P < 0.05$ vs. respective control; **, $P < 0.05$ vs. control WT mice; †, $P < 0.05$ vs. diabetic WT mice.

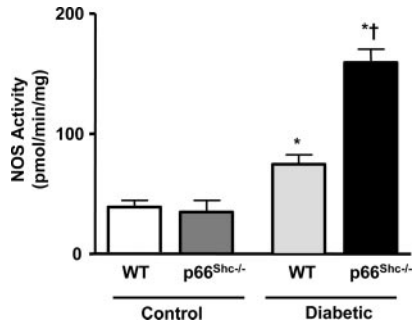

Fig. 8. NOS activity in WT and $p66^{Shc-/-}$ mice under control and diabetic conditions. Results are presented as mean ± SEM; $n = 6$ in each group. *, $P < 0.05$ vs. respective control; †, $P < 0.05$ vs. diabetic WT mice.

PHYSIOLOGY

peroxidase-conjugated anti-mouse/rabbit Ig antibody (1:2,000; Amersham Pharmacia Biotech, Piscataway, NJ)], and protein expression was detected by enhanced chemiluminescence kit (ECL Plus; Amersham Pharmacia Biotech). Anti-α-tubulin mouse monoclonal antibody (1:2,000; Sigma–Aldrich) was used for equal loading control. Western blots were quantified densitometrically by using the public domain NIH Image 1.6 program developed by the National Institutes of Health (Bethesda, MD).

Measurement of $ONOO^-$. $ONOO^-$ generation in aortic tissue was determined by using chemiluminescence detection with the luminal analog L-012. Each tissue sample (5-mm length) was placed into 1 ml of modified Krebs–Ringer solution (pH 7.4) and incubated at 37°C for 1 h under a supply of carbogen. Immediately before measurement, rings were transferred into scintillation tubes filled with 500 μl of Krebs–Hepes solution (pH 7.4) at 37°C. L-012 was added to give a final concentration of 100 μM.

Chemiluminescence of L-012 was detected with a thermostated single tube luminometer FB12 (Berthold Detection Systems, Oak Ridge, TN) and expressed as relative light units per second.

Immunohistochemical Detection of 3-Nitrotyrosine. Thoracic aorta segments from all mice were embedded in optimum cutting temperature and stored at −80°C. Five-micrometer-thick slices were then cut, blocked with PBS/1% BSA for 1 h, and incubated for 1 h at room temperature with anti-nitrotyrosine rabbit polyclonal antibody (5 μg/ml dilution; Upstate Biotechnology). Thereafter, fluorescence-labeled secondary antibody (Molecular Probes, Eugene, OR) was applied for 1 h (1:200). Successively, slides were rinsed with PBS and embedded in Immu-Mount for fluorescence microscopy with a Leica (Nidau, Switzerland) DMIRB equipped with a digital spot camera (Visitron System; Visitron, Puchheim, Germany).

TBARS Assay. *In vitro* assessment of aortic levels of lipid peroxidation was performed by using a TBARS assay kit (OXItek; ZeptoMetrix, Buffalo, NY), according to the manufacturer's instructions. Briefly, snap-frozen tissue was crushed in a prechilled mortar and pestle and resuspended at a concentration of 50 mg/ml in PBS. One hundred microliters of homogenate was then added to the SDS solution and mixed thoroughly. After the addition of the TBA/buffer reagent, samples were incubated at 95°C for 60 min. After incubation, samples were brought back to room temperature and centrifuged at 956 $\times$ *g* for 15 min. Absorbance was then read at 532 nm.

Measurement of NOS and HO Activity. Frozen aortic rings were homogenized in PBS. Samples were then centrifuged at 45,000 rpm at 4°C for 20 min. NOS activity was measured by the conversion of L-[^{14}C]arginine to L-[^{14}C]citrulline and expressed as picomoles per μg of protein per minute. Forty microliters of supernatant was incubated for 30 min at 37°C with 40 μl of assay buffer containing 32.3 mM Hepes, 0.8% glycerol, 5 μM L-arginine (Sigma, St. Louis, MO), 6 μM FAD (Sigma), 6 μM FMN (Sigma), 100 units/ml calmodulin (Bio-Mol, Plymouth, PA), 3 mM DTT (Lancaster, U.K.), 5 μM L-[^{14}C]arginine (Amersham Pharmacia Biotech), and 250 μM NADPH (Bio-Mol). Incubations were performed in the presence and in the absence of 1 mmol/liter EGTA to determine both the Ca^{2+}-dependent and -independent formation of citrulline. After 30 min, the reaction was stopped by the addition of 120 μl of methanol. One hundred microliters of the mixture was spotted by glass capillaries onto a silica TLC plate (Silica 60; Merck, Darmstadt, Germany) and subjected to chromatography. The solvent consisted of 30% ammonium hydroxide/chloroform/methanol/water in a 2:0.5:4.5:1 mixture. Plates were exposed to a PhosphorImager screen overnight. For reading the screen, a PhosphorImager system (Molecular Dynamics, Sunnyvale, CA) was used. Quantification was performed by using ImageQuant software.

HO activity was measured as production of total free bilirubin (Chema Diagnostica, Jesi, AN, Italy). Bilirubin reacts with diazotized sulfanilic acid to produce an intensely colored diazo dye (490–520 nm). The intensity of color of this dye in solution with the sample is proportional to the concentration of total bilirubin. One hundred microliters of sample was added to the dye, mixed, and incubated for 5 min at 37°C. Absorbance was then measured at 510 nm (interval allowed was 490 ÷ 520 nm) with the use of a spectrophotometer. Readings were then normalized against reagent blank and calibrator.

Statistical Analysis. In all experiments, *n* equals the number of mice for the experiment. Results are expressed as mean ± SEM. Statistical evaluations of the data were performed by using an unpaired Student's *t* test or ANOVA followed by Bonferroni post hoc corrections as appropriate. A value of $P < 0.05$ was considered statistically significant.

This work was supported in part by Swiss National Research Foundation Grants 310000108463 (to F.C.), 3100068118.02 (to T.F.L.), Italian MIUR-PRIN 2004069574_002 (to F.C.), and a grant from the Swiss Heart Foundation. M.S. was the recipient of a fellowship from the Italian Society of Arterial Hypertension.

1. Creager MA, Luscher TF, Cosentino F, Beckman JA (2003) *Circulation* 108:1527–1532.
2. Widlansky ME, Gokce N, Keaney JF, Jr, Vita JA (2003) *J Am Coll Cardiol* 42:1149–1160.
3. Lerman A, Zeiher AM (2005) *Circulation* 111:363–368.
4. van der Loo B, Labugger R, Skepper JN, Bachschmid M, Kilo J, Powell JM, Palacios-Callender M, Erusalimsky JD, Quaschning T, Malinski T, *et al.* (2000) *J Exp Med* 192:1731–1744.
5. Turko IV, Murad F (2002) *Pharmacol Rev* 54:619–634.
6. Cosentino F, Hishikawa K, Katusic ZS, Luscher TF (1997) *Circulation* 96:25–28.
7. Cosentino F, Eto M, De Paolis P, van der Loo B, Bachschmid M, Ullrich V, Kouroedov A, Delli Gatti C, Joch H, Volpe M, Luscher TF (2003) *Circulation* 107:1017–1023.
8. Bonfini L, Migliaccio E, Pelicci G, Lanfrancone L, Pelicci PG (1996) *Trends Biochem Sci* 21:257–261.
9. Migliaccio E, Giorgio M, Mele S, Pelicci G, Reboldi P, Pandolfi PP, Lanfrancone L, Pelicci PG (1999) *Nature* 402:309–313.
10. Napoli C, Martin-Padura I, de Nigris F, Giorgio M, Mansueto G, Somma P, Condorelli M, Sica G, De Rosa G, Pelicci P (2003) *Proc Natl Acad Sci USA* 100:2112–2116.
11. Francia P, delli Gatti C, Bachschmid M, Martin-Padura I, Savoia C, Migliaccio E, Pelicci PG, Schiavoni M, Luscher TF, Volpe M, Cosentino F (2004) *Circulation* 110:2889–2895.
12. Trinei M, Giorgio M, Cicalese A, Barozzi S, Ventura A, Migliaccio E, Milia E, Padura IM, Raker VA, Maccarana M, *et al.* (2002) *Oncogene* 21:3872–3878.
13. Orsini F, Migliaccio E, Moroni M, Contursi C, Raker VA, Piccini D, Martin-Padura I, Pelliccia G, Trinei M, Bono M, *et al.* (2004) *J Biol Chem* 279:25689–25695.
14. Nemoto S, Finkel T (2002) *Science* 295:2450–2452.
15. Giorgio M, Migliaccio E, Orsini F, Paolucci D, Moroni M, Contursi C, Pelliccia G, Luzi L, Minucci S, Marcaccio M, *et al.* (2005) *Cell* 122:221–233.
16. Nishikawa T, Edelstein D, Du XL, Yamagishi S, Matsumura T, Kaneda Y, Yorek MA, Beebe D, Oates PJ, Hammes HP, *et al.* (2000) *Nature* 404:787–790.
17. Pagnin E, Fadini G, de Toni R, Tiengo A, Calo L, Avogaro A (2005) *J Clin Endocrinol Metab* 90:1130–1136.
18. Menini S, Amadio L, Oddi G, Ricci C, Pesce C, Pugliese F, Giorgio M, Migliaccio E, Pelicci P, Iacobini C, Pugliese G (2006) *Diabetes* 55:1642–1650.
19. Pieper GM, Meier DA, Hager SR (1995) *Am J Physiol* 269:H845–H850.
20. Johnstone MT, Creager SJ, Scales KM, Cusco JA, Lee BK, Creager MA (1993) *Circulation* 88:2510–2516.
21. Ting HH, Timimi FK, Boles KS, Creager SJ, Ganz P, Creager MA (1996) *J Clin Invest* 97:22–28.
22. McVeigh GE, Brennan GM, Johnston GD, McDermott BJ, McGrath LT, Henry WR, Andrews JW, Hayes JR (1992) *Diabetologia* 35:771–776.
23. Ortiz A, Lorz C, Justo P, Catalan MP, Egido J (2001) *J Cell Mol Med* 5:18–32.
24. Matsuoka T, Wada J, Hashimoto I, Zhang Y, Eguchi J, Ogawa N, Shikata K, Kanwar YS, Makino H (2005) *Diabetes* 54:2882–2890.
25. White CR, Brock TA, Chang LY, Crapo J, Briscoe P, Ku D, Bradley WA, Gianturco SH, Gore J, Freeman BA, *et al.* (1994) *Proc Natl Acad Sci USA* 91:1044–1048.
26. Kurosawa T, Itoh F, Nozaki A, Nakano Y, Katsuda S, Osakabe N, Tsubone H, Kondo K, Itakura H (2005) *Atherosclerosis* 179:237–246.
27. Abraham NG, Kushida T, McClung J, Weiss M, Quan S, Lafaro R, Darzynkiewicz Z, Wolin M (2003) *Circ Res* 93:507–514.
28. Foresti R, Clark JE, Green CJ, Motterlini R (1997) *J Biol Chem* 272:18411–18417.
29. Hayashi S, Takamiya R, Yamaguchi T, Matsumoto K, Tojo SJ, Tamatani T, Kitajima M, Makino N, Ishimura Y, Suematsu M (1999) *Circ Res* 85:663–671.
30. Nath KA, Haggard JJ, Croatt AJ, Grande JP, Poss KD, Alam J (2000) *Am J Pathol* 156:1527–1535.
31. Stocker R, Yamamoto Y, McDonagh AF, Glazer AN, Ames BN (1987) *Science* 235:1043–1046.
32. Yachie A, Niida Y, Wada T, Igarashi N, Kaneda H, Toma T, Ohta K, Kasahara Y, Koizumi S (1999) *J Clin Invest* 103:129–135.
33. Goodman AI, Chander PN, Rezzani R, Schwartzman ML, Regan RF, Rodella L, Turkseven S, Lianos EA, Dennery PA, Abraham NG (2006) *J Am Soc Nephrol* 17:1073–1081.
34. Liu X, Wei J, Peng DH, Layne MD, Yet SF (2005) *Diabetes* 54:778–784.
35. Quan S, Kaminski PM, Yang L, Morita T, Inaba M, Ikehara S, Goodman AI, Wolin MS, Abraham NG (2004) *Biochem Biophys Res Commun* 315:509–516.
36. Zaccagnini G, Martelli F, Fasanaro P, Magenta A, Gaetano C, Di Carlo A, Biglioli P, Giorgio M, Martin-Padura I, Pelicci PG, Capogrossi MC (2004) *Circulation* 109:2917–2923.
37. Casselli DS, Martins LR (2006) *J Adhes Dent* 8:53–58.